American Mineralogist, Volume 78, pages 769–774, 1993

Partially disordered dolomite: Microstructural characterization of Abu Dhabi sabkha carbonates

HANS-RUDOLF WENK, HU MEISHENG
Department of Geology and Geophysics, University of California, Berkeley, California 94720, U.S.A.
SILVIA FRISIA
Dipartimento di Scienze della Terra, Università degli Studi, Via Mangiagalli 34, 20133 Milano, Italy

ABSTRACT

Transmission and analytical electron microscopy observations document at least three carbonate phases in sediments of the Abu Dhabi sabkha: aragonite, ordered dolomite often showing modulated microstructure, and a mostly disordered calcium magnesium carbonate with submicrometer-sized ordered domains. It is suggested that ordered and partially ordered dolomite formed mainly by direct precipitation from pore fluids, with changing temperature and chemistry in response to environmental parameters.

INTRODUCTION

An important question in carbonate sedimentology is whether early dolomitization by marine waters occurs by means of precipitation of ordered dolomite or if the first precipitate is a disordered calcium magnesium carbonate, which later transforms to ordered dolomite during diagenesis. We contribute to this discussion by characterizing Holocene carbonates from the coastal sabkha of Abu Dhabi with the transmission electron microscope (TEM). For the diagenetic sediments of the Abu Dhabi sabkha, an early dolomitization model has been proposed and may provide an important modern analogue for ancient massive dolostones associated with evaporites (McKenzie, 1990).

The mechanism of dolomite precipitation (primary vs. replacement of former unstable carbonate phases) and the relationships between dolomite and other carbonates have mainly been characterized by XRD and bulk chemical analysis. Microstructures, as observed with the TEM, combined with phase identification, can provide further information about the parent fluid composition and the mechanisms of dolomitization in recent sediments. Other arid settings produce poorly ordered dolomite with a high defect density (Rosen et al., 1989). Their presence in the Abu Dhabi sabkha sediments would be indicative of complex diagenesis in the presence of fluids with variable compositions and degrees of saturation.

The scope of this study is to (1) identify the carbonate phases present and describe their structure, composition, and morphology; (2) investigate the relationships between ordered dolomite and unstable carbonates, in particular the evidence of replacement features at grain boundaries between dolomite and aragonite; (3) infer from these observations early dolomitization mechanisms in a recent sabkha setting.

EXPERIMENTAL PROCEDURES

In this study we observed and analyzed Holocene dolomite samples from the upper intertidal, lower intertidal, and subtidal facies of the Abu Dhabi sabkha described by McKenzie (1981; her Fig. 2). The samples are the same as those used in a recent Sr isotope investigation (Müller et al., 1990). Sediments containing between 40 and 60 vol% dolomite were first examined by conventional optical microscopy and then with a Cambridge scanning electron microscope (SEM) in order to characterize the morphology of the dolomite crystals and their spatial relationships with other carbonates and to visually estimate dolomite abundance. Dolomite is more common in subtidal facies sediments (samples AD 32 in Fig. 2 of Müller et al., 1990), where it appears as coalescing aggregates of rhombs (Fig. 1).

Preliminary X-ray diffraction analysis of powders of subtidal samples revealed that aragonite peaks dominate, and their large intensities make it difficult to identify dolomite and calcite peaks. Therefore, the method was unsatisfactory for characterizing the mineralogical composition of the sediment. Subsequently, TEM specimens were prepared in such a way as to preserve as much as possible the original textural relationships. Loose sand-sized grains and mud were embedded in epoxy, and then a standard petrographic thin section was prepared. Selected areas of interest, as observed with the petrographic microscope, were mounted on a Cu grid, detached from the glass support, and thinned to electron transparency by ion milling. With this method, TEM foils better reflect the natural distribution of dolomite in unconsolidated sediments than if powders are used. A routine survey was conducted with a JEM 100C TEM in the Department of Geology and Geophysics. Areas of interest were then characterized with more advanced instruments at the National Center for

0003–004X/93/0708–0769$02.00

Fig. 1. SEM image of an intertidal carbonate assemblage from the Abu Dhabi sabkha (AD 31). Shown are aragonite needles and dolomite and magnesian calcite rhombs.

Electron Microscopy (NCEM) at the Lawrence Berkeley Laboratory. An analytical Jeol JEM 200 CX STEM equipped with a LaB_6 filament, a high-angle X-ray detector, and a KEVEX EDX system (AEM) served for chemical microanalyses for Ca, Mg, Sr, Fe, and Na. The consistency of the AEM data was subsequently checked by electron microprobe analyses using an ARL microprobe with a beam diameter of about 2 μm on samples. Analyses were performed on dolomite grains that were large enough to be entirely in the analytical volume of the probe. AEM and microprobe values of major elements were generally consistent. On some samples the Jeol ARM 1000 atomic resolution microscope was used to resolve fine structural details.

Observations

Two samples from the intertidal facies (AD 30 and AD 31) consist of loose, light gray carbonate mud and fine sand composed of bioclasts and peloids, the size of which is generally <100 μm. Dolomite rhombs are very small and mostly occur in intergranular pores as cement.

Subtidal samples (AD 32 and AD 79) are coarser grained, loose carbonate sand, mostly composed of peloids and subordinate bioclasts such as gastropod fragments and algal debris, the size of which exceeds 400 μm. In the subtidal samples that we investigated, dolomite is more common than in the intertidal samples. It occurs both as intergranular cement and as intragranular products of dissolution and reprecipitation.

When imaged with the SEM, dolomite appeared in all the samples as euhedral crystals 0.1–2 μm in size. It occurs in pores 3–4 μm in diameter within a mesh of euhedral aragonite needles 1–2 μm long (Fig. 1). Intragranular porosity is very high. In addition, in subtidal facies, dolomite rhombs start to coalesce to form larger aggregates, up to 5 μm in size, and relationships with aragonite are less clear. Aragonite is still largely euhedral but partially incorporated within rhombs. Intragranular porosity is lower than in the intertidal facies.

With the TEM at least three carbonate phases could be identified: aragonite, dolomite with an ordered cation distribution, and magnesian calcite grading into dolomite with a partially ordered cation distribution. Figure 2a shows fine euhedral aragonite needles, easily recognized by pervasive {110} twinning and a characteristic diffraction pattern. These needles surround dolomite rhombs, which are up to 2 μm wide in a subtidal sample (Fig. 2b). Dolomite and aragonite are intimately intergrown, with aragonite needles <100 nm wide penetrating dolomite rhombs and composing at least 1% of the dolomite volume (Fig. 2c). Microporosity is common at grain boundaries and also within dolomite rhombs. Although in intertidal samples dolomite and euhedral aragonite coexist without evidence for resorption surfaces, in subtidal facies some larger aragonite crystals show indented irregular surfaces at contacts with dolomite rhombs (Fig. 2d). These can be considered as evidence of dissolution of aragonite and replacement by dolomite. Very small aragonite inclusions (only tens of nanometers in size) persist in larger dolomite grains, and irregular boundaries suggest that aragonite has been partially replaced.

In all the different facies, ordered dolomite is quite heterogeneous, with a mottled contrast that is often present as a well-developed, planar, modulated structure (Fig. 3a), reminiscent of the $10\bar{1}4$ modulated structure frequently observed in low-temperature calcian dolomite (e.g., Wenk et al., 1983). Diffraction patterns illustrate that dolomite is ordered, with reflections such as 0003 and $01\bar{1}5$ present. In the diffraction pattern illustrated in Figure 3a, the presence of these spots cannot be due to double diffraction. The composition, as determined with the AEM, is $Ca_{0.54}Mg_{0.46}CO_3$ and fairly uniform at the scale of a 200-nm AEM probe.

The ordered dolomite crystals from intertidal samples are internally heterogeneous with strain contrast and domains of differently developed lamellar microstructures, resembling agglomerates, but diffraction patterns are coherent. Composition determined by AEM is variable within some domains that contain up to 3% excess Mg. Conceivably there could be magnesite inclusions. In none of the dolomite crystals did we observe c-superstructure reflections, which are common in ancient calcian dolomite (e.g., Wenk et al., 1991), but have also been observed in some recent dolomite (Mitchell et al., 1987).

Also of rhombohedral morphology is a disordered magnesium calcium carbonate of variable composition in the range of $Ca_{0.7}Mg_{0.3}CO_3$ (Fig. 3b), with ordering reflections either attenuated or absent in the diffraction pattern. In this magnesian calcite we also observe a heterogeneous microstructure; however, it is less regular than in ordered dolomite.

The samples have been investigated with the ARM to obtain more information about structural details. The investigation was difficult because of substantial radiation

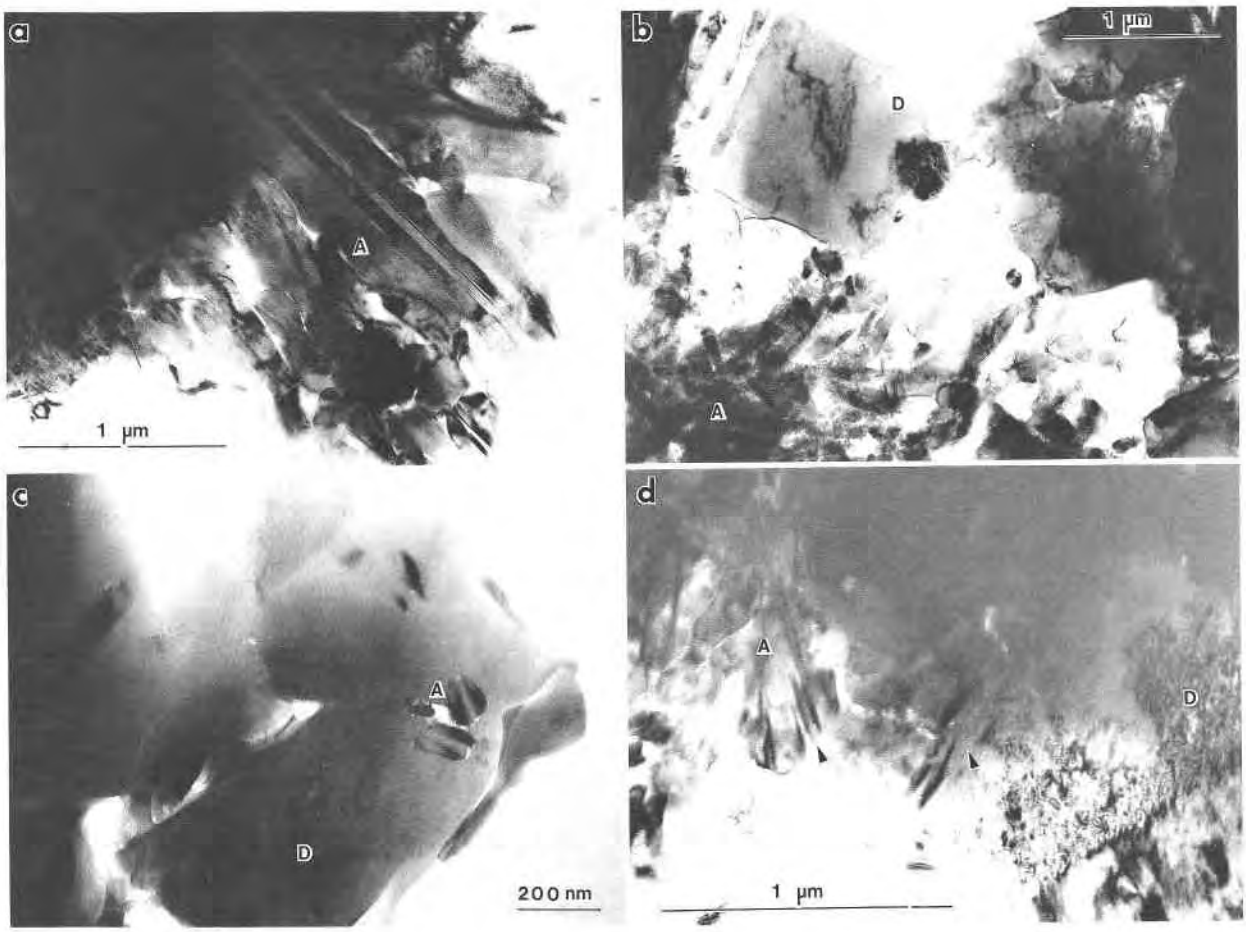

Fig. 2. TEM electron micrographs of aragonite and dolomite. (**a**) Aragonite needles, some of them displaying {110} twinning. (**b**) Dolomite rhombs surrounded by aragonite (AD 79). (**c**) Dolomite rhomb (D) with minute aragonite inclusions (A). (**d**) Dolomite (D) and aragonite (A) with indented faces (arrow), indicative of dissolution (AD 32).

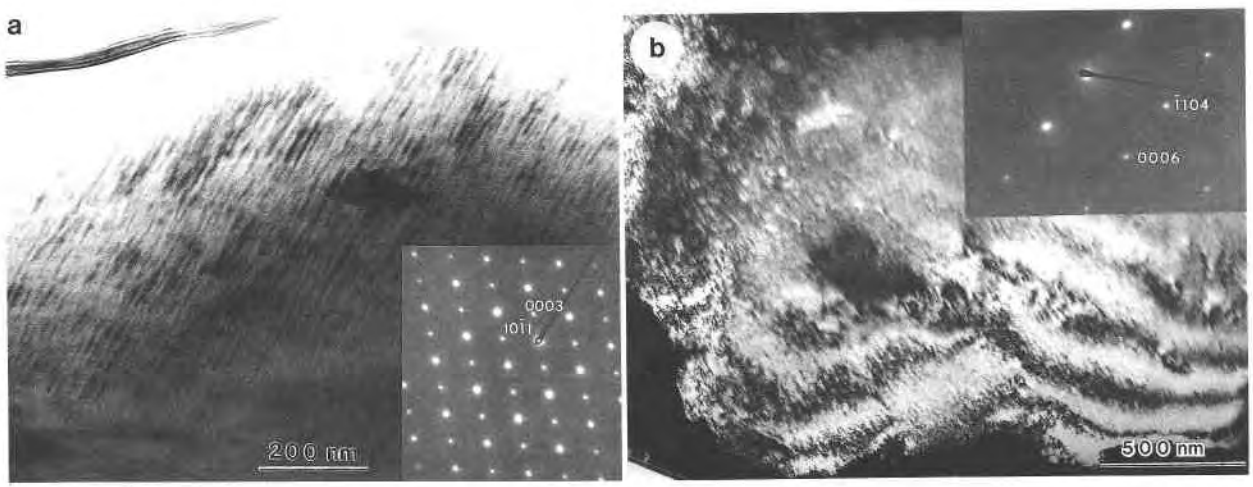

Fig. 3. Rhombohedral carbonates in Abu Dhabi sabkha. (**a**) Calcian dolomite with modulated microstructure parallel to $(10\bar{1}4)$. The inserted diffraction pattern shows that the dolomite is fully ordered. (**b**) Magnesian calcite. In the diffraction pattern the (0003) ordering reflection is absent.

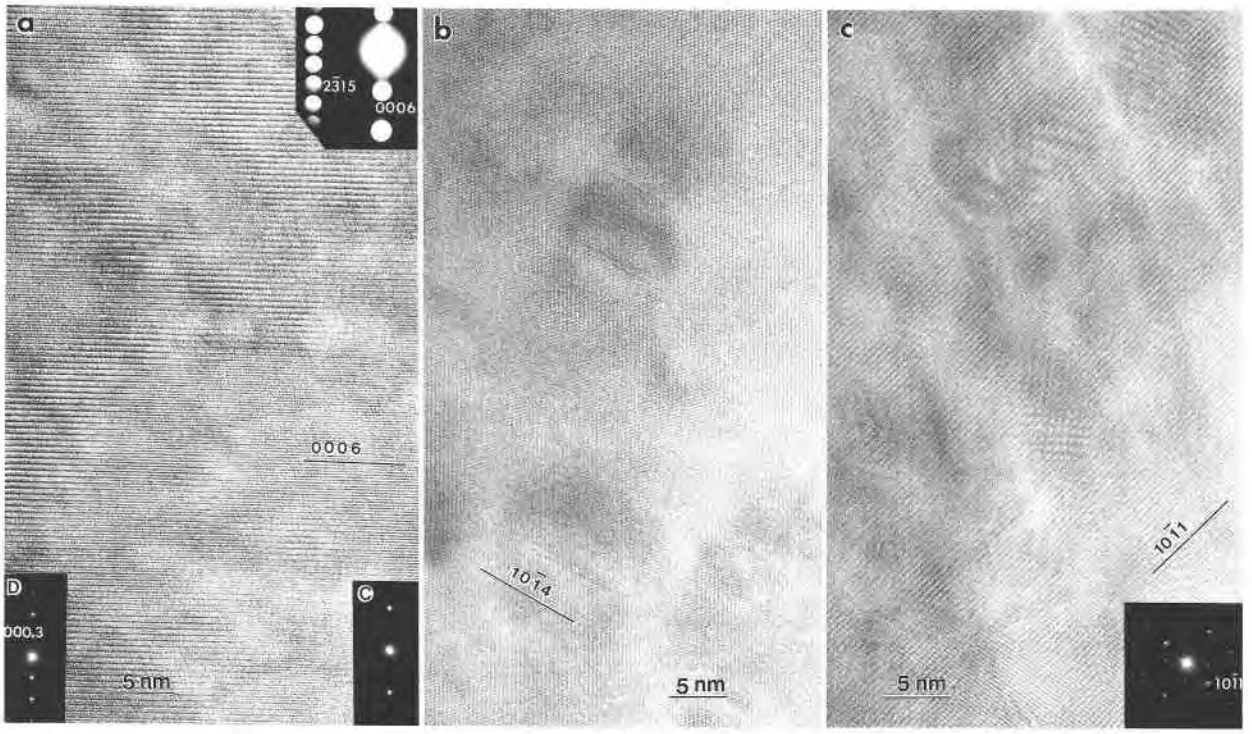

Fig. 4. Atomic resolution phase-contrast images of magnesian calcite in AD 79. (**a**) Magnesian calcite with spherical domains of ordered dolomite. The diffraction pattern (top right) shows highly attenuated ordering reflections. In optical diffractograms of most of the areas, ordering reflections are absent (C); however, some regions display dolomite layer ordering (D). (**b**) View onto {10$\bar{1}$4} lattice planes with local platelike defects, which may represent GP zones of different composition. (**c**) Highly irregular fine mosaic structure with domains, which are in slightly different orientation, as evidenced by moiré fringes.

damage occurring in the electron beam (Van Tendeloo et al., 1985). However, it was possible to obtain some interesting results with multibeam phase contrast images (Fig. 4a–4c). Most of the crystal in Figure 4a is disordered, with regular basal (0006) fringes. In some areas, however, there is a doubling of the basal repeat (0003), indicative of local Mg and Ca ordering in alternate basal layers. The ordered spherical domains are only 2–10 nm in diameter. We ascertained that the domain structure is real and not a result of damage by comparing images from through-focus series, taken during about 2 min of exposure. The morphology and structure of the domains did not change during that period. We have ruled out the possibility that the changes in contrast could be due to variations in foil thickness or orientation because the areal extent is very small.

The electron diffraction pattern, as obtained from an area approximately 200 nm in diameter, shows no ordering reflections (inserted in Fig. 4a). However, on laser-optical diffractograms obtained using the image negatives, we observed dolomite ordering in these domains. Diffractograms from ordered regions (D) and disordered regions (C) are inserted in Figure 4a. The spacing of basal fringes in the disordered and ordered regions is similar, and there is no splitting of reflections in a diffractogram taken over a larger region, including ordered and disordered areas. This indicates that the compositions are similar, which was also confirmed by direct AEM analysis. Calcite has a d_{0001} value that is 8% larger than that of dolomite, and such a difference could be easily resolved in the diffractogram (Wenk et al., 1991). Ordered dolomite precipitates are coherent overall. In a different view of the structure (Fig. 4b), we observe (10$\bar{1}$4) fringes. The regular fringe pattern is interrupted by faults that extend about 10 nm. They appear as thin platelets and may represent Guinier-Preston zones, with local deviations in composition. The (10$\bar{1}$4) orientation is parallel to a modulation observed in low magnification micrographs (Fig. 3b). Apart from these defects and ordered domains, magnesian calcite crystals are fairly homogeneous. However, in some areas there are considerable distortions due to internal strain and misorientations of small domains. The mosaic structure is particularly visible in the {10$\bar{1}$1} lattice fringes (Fig. 4c). Strain introduces complicated moiré fringe patterns.

Semiquantitative AEM analyses indicate that aragonite contains about 7000 ppm Sr, independently of its occurrence as loose needles or as inclusions within dolomite. The local Sr content of magnesium calcite is about 500 ppm, and that of ordered dolomite <200 ppm, which is slightly less than that described in other recent dolomite (Mitchell et al., 1987). Small amounts of Na (100–300

ppm) are present, especially in intertidal dolomite with high defect densities. Na may be concentrated at crystal defects, as suggested by Busenberg and Plummer (1985), or may occur as small inclusions of halite.

Discussion

There is no consensus regarding the nature of controls on calcium magnesium carbonate crystallization in sedimentary environments, particularly the issue of direct crystallization vs. replacement (e.g., Zenger et al., 1980). Our data do not resolve this problem but add some constraints. Experimental data at low temperature (33 °C) suggest the importance of a high Mg/Ca ratio in pore waters for the formation of Ca-rich disordered dolomite (Oomori and Kitano, 1987). Local nucleation of more ordered carbonates can also be the result of kinetic factors and temperature (Morse and MacKenzie, 1990) or of the influence of surface chemistry on growth (Paquette and Reeder, 1990). Dolomitization experiments indicate that a high Mg/Ca activity ratio (Sibley et al., 1987) and an elevated HCO_3^- concentration kinetically favor rapid nucleation and the growth of ideal and moderately ordered dolomite with sporadic occurrence of magnesite (Morrow and Ricketts, 1988). It is possible that temporal changes in H_2O composition, induced by a variety of factors, including seasonal changes, may account for the coexistence of diverse carbonate phases in Abu Dhabi sabkha sediments. McKenzie et al. (1980) documented pore fluid chemistry changes in response to environmental conditions, such as periodic marine floodings and evaporative periods.

TEM observations document the presence of ordered calcian dolomite in Holocene carbonates from the coastal sabkha of Abu Dhabi. The euhedral crystals precipitated from saline brines and are not detrital. There is evidence for minor replacement of aragonite. Ca-Mg ordering occurred most probably during initial growth, and we consider this observation as most significant. A second calcium magnesium carbonate, of similar morphology and a slightly more calcic composition, has a largely disordered Ca-Mg distribution but with small ordered domains.

Disordered calcium magnesium carbonates are restricted to recent sediments, whereas ancient magnesian calcite contains coherent domains with different superstructures (e.g., Reksten, 1990; Wenk et al., 1991). It appears that ordered dolomites are generally not caused by ordering of a disordered protodolomite but are the result of direct growth, largely by dissolution and reprecipitation. It appears that dolomitization of the Abu Dhabi sabkha diagenetic sediments occurred mainly by direct precipitation of ordered and disordered dolomite from saline solutions. Only locally was aragonite replaced by dissolution and reprecipitation. Both mechanisms occur simultaneously during early diagenesis. Similar agglomerates of disordered calcium magnesium carbonates, observed in the sediments of the Coorong region (Rosen et al., 1989), are interpreted as having precipitated from evaporating brines, which provide both the cations and anions necessary for direct precipitation.

The TEM observations also illustrate heterogeneity on a very fine scale, which puts limitations on bulk analytical methods such as X-ray powder diffraction and geochemical analyses, including electron microprobe analyses, which average over different phases. For example, Sr isotopes have been used to test dolomitization models, and these analyses rely on mechanically or chemically separated powders. In the case of the Abu Dhabi samples, it is impossible to separate microinclusions of aragonite, only 10 nm wide, from surrounding dolomite. Since Sr is enriched by a factor of 10–20 in aragonite, contributions from these inclusions, which constitute 1–5 vol%, may interfere with the Sr isotope signature. As a consequence, Sr isotopes may reflect mostly the composition of the fluids from which aragonite, rather than dolomite, precipitated. This further demonstrates that TEM characterization and AEM chemical analyses are indispensable in the study of the diagenetic mechanisms that transform a carbonate sediment into a stable limestone or dolostone.

Acknowledgments

We are appreciative for generous access to the facilities of NCEM-LBL. We wish to thank C. Ecker for help with AEM, J. Donovan for microprobe analyses, and T. Tigue for his skills in preparing delicate thin sections. The authors are grateful to J.A. McKenzie and D. Müller for providing samples and information about settings and geochemistry. We profited from valuable discussions and comments on the manuscript by J. Christensen, J.A. McKenzie, D.E. Miser, and R.J. Reeder. S.F. was supported by a grant to F. Jadoul (Milan), whose constant encouragement is acknowledged. H.M. and H.R.W. are appreciative of the support of the University of California Education Abroad program and NSF grant EAR-91-04605.

References cited

Busenberg, E., and Plummer, L.N. (1985) Kinetic and thermodynamic factors controlling the distribution of SO_4^{2-} and Na^+ in calcites and selected aragonites. Geochimica et Cosmochimica Acta, 49, 713–725.

McKenzie, J.A. (1981) Holocene dolomitization of calcium carbonate sediments from the coastal sabkhas of Abu Dhabi, U.A.E.: A stable isotope study. Journal of Geology, 89, 185–198.

——— (1990) Dolomites: Reconciling a modern example with the ancient record. Chemical Geology, 84, 190–191.

McKenzie, J.A., Hsu, K.J., and Schneider, J.F. (1980) Movement of subsurface waters under the sabkha, Abu Dhabi, UAE, and its relation to evaporative dolomite genesis. In D.H. Zenger, J.B. Dunham, and R.L. Ethington, Eds., Concepts and models of dolomitization, p. 11–30. Society of Economic Paleontologists and Mineralogists, Tulsa, Oklahoma.

Mitchell, J.T., Land, L.S., and Miser, D.E. (1987) Modern marine dolomite cement in a north Jamaican fringing reef. Geology, 15, 557–560.

Morrow, D.W., and Ricketts, B.D. (1988) Experimental investigation of sulfate inhibition of dolomite and its mineral analogues. In V. Shukla and P.A. Baker, Eds., Sedimentology and geochemistry of dolostones, p. 25–38. Society of Economic Paleontologists and Mineralogists, Tulsa, Oklahoma.

Morse, J.W., and MacKenzie, F.T. (1990) Geochemistry of sedimentary carbonates, 707 p. Elsevier, Amsterdam.

Müller, D.W., McKenzie, J.A., and Mueller, P.A. (1990) Abu Dhabi sabkha Persian Gulf, revisited: Application of strontium isotopes to test an early dolomitization model. Geology, 18, 618–621.

Oomori, T., and Kitano, Y. (1987) Synthesis of protodolomite from seawater containing dioxane. Geochemical Journal, 21, 59–65.

Paquette, J., and Reeder, R.J. (1990) New type of compositional zoning in calcite: Insights into crystal-growth mechanisms. Geology, 18, 1244–1247.

Reksten, K. (1990) Superstructures in calcite. American Mineralogist, 75, 807–812.

Rosen, M.R., Miser, D.E., Starcher, M.A., and Warren, J.K. (1989) Formation of dolomite in the Coorong region, South Australia. Geochimica et Cosmochimica Acta, 53, 661–669.

Sibley, D.F., Dedoes, R.E., and Bartlett, T.R. (1987) Kinetics of dolomitization. Geology, 15, 1112–1114.

Van Tendeloo, G., Wenk, H.-R., and Gronsky, R. (1985) Modulated structures in calcian dolomite: A study by electron microscopy. Physics and Chemistry of Minerals, 12, 333–341.

Wenk, H.-R., Barber, D.J., and Reeder, R.J. (1983) Microstructures in carbonates. In Mineralogical Society of America Reviews in Mineralogy, 11, 301–361.

Wenk, H.-R., Meisheng, H., Lindsey, T., and Morris, W. (1991) Superstructures in ankerite and calcite. Physics and Chemistry of Minerals, 17, 527–539.

Zenger, D.H., Dunham, J.B., and Ethington, R.L. (1980) Concepts and models of dolomitization. Society of Economic Paleontologists and Mineralogists Special Publication, 28, 426 p.

Manuscript received March 10, 1992
Manuscript accepted March 24, 1993